

**DEVICE PHYSICS OF THIN-FILM
POLYCRYSTALLINE CELLS AND MODULES**

Phase I
Annual Report

February 1998 - January 1999

by

James R. Sites
Department of Physics
Colorado State University
Fort Collins CO 80523

Work performed Under Subcontract XAK-8-17619-07
National Renewable Energy Laboratory
1617 Cole Boulevard
Golden Colorado 80401

SUMMARY

Work has continued at Colorado State to make basic measurements on CI(G)S and CdTe solar cells fabricated at different labs, to quantitatively deduce the loss mechanisms in these cells, and to make appropriate comparisons that illuminate where progress is being made. Cells evaluated included the new record CIGS cell, CIS cells made with and without CdS, and those made by electrodeposition and electroless growth from solution.

A second area of emphasis, the role of impurities, has focused on sodium in CIS. Cells with varying amounts of sodium added during CIS deposition were fabricated at NREL using four types of substrates. Best performance was achieved with 10^{-2} – 10^{-1} at% sodium, and the relative merits of proposed mechanisms for the sodium effect were compared.

A new area of work has been the construction and testing of fine-focused laser-beam apparatus to measure local variations in polycrystalline cell performance. A 1 μm spot has been achieved, spatial reproducibility in one and two dimensions is less than 1 μm , and photocurrent is reliably measured when the 1 μm spot is reduced as low as 1 sun in intensity.

Elevated-temperature stress tests have been performed on both CdTe and CIS cells. Typical CdTe cells held at 100° C under illumination and normal resistive loads for extended periods of time were generally very stable, but those held under reverse or large forward bias and those contacted using larger amounts of copper were somewhat less stable.

Modeling of CdTe cells has produced reasonable fits to experimental data including variations in back contact barriers. A major challenge being addressed is the photovoltaic response of a single simple-geometry crystallite with realistic grain boundaries.

TABLE OF CONTENTS

SUMMARY	i
FIGURES/TABLES	iii
INTRODUCTION.....	1
LOSS ANALYSIS	2
IMPURITY EFFECTS.....	6
SMALL-SPOT MEASUREMENT.....	10
STRESS TESTS.....	14
MODELING	18
COMMUNICATIONS.....	21
Publications	21
Graduate Degrees	21
Reports	22

FIGURES

Figure 1. J-V comparison of record CIGS cell	2
Figure 2. J-V comparison with varying Na.....	7
Figure 3. Variation in V_{oc} with Na	7
Figure 4. Variation in hole density with sodium.....	8
Figure 5. Schematic of small-spot stepping apparatus.....	10
Figure 6. Linear scans of 30 μm slit and 20 μm grid.....	11
Figure 7. Response to 1 μm spot with varying intensity.....	12
Figure 8. J-V for CdTe exposed to 100° C for 1000 hr.....	15
Figure 9. Stress test C-V for CdTe.....	16
Figure 10. CIS light/dark transient.....	17
Figure 11. Initial CdTe profile used in modeling.....	18
Figure 12. 2D CdTe picture with model single grain.....	19

TABLES

Table I. Comparison of NREL CIGS cells.....	3
Table II. Device parameters of ED and EL cells	4
Table III. Device parameters of CdS and non-CdS cells	5

INTRODUCTION

The objectives of the Colorado State University (CSU) program are to (1) quantitatively separate individual performance losses in CI(G)S and CdTe solar cells using currently available techniques, (2) expand the tool set for measuring and separating the losses, and (3) suggest fabrication approaches or modifications to minimize the losses.

Most of the experimental and analytical work has been done by two dedicated research students, Jennifer Granata, who finished her Ph.D. in December 1998 and now works at Spectrolab, and Jason Hiltner who completed his M.S. in May 1998, and is working full-time towards his Ph.D. In addition, graduate student Ajit Dhamdhare and undergraduate Yvonne Shelton have done individual projects, engineer David Warner has designed and built part of the new apparatus, and senior research collaborator Alan Fahrenbruch has had a productive year with computer-based modeling.

The Colorado State group has been an active part of the NREL-sponsored National CdTe and CIS R&D Teams. It has had active collaborations with researchers at the Colorado School of Mines, Global Solar, Inc., the Institute of Energy Conversion, International Solar Electric Technology, Inc., the National Renewable Energy Laboratory, Siemens Solar Industries, Solar Cells, Inc., the University of South Florida, the University of Toledo, and Washington State University.

LOSS ANALYSIS

There were four explicit loss analysis projects during Phase I, all involving or related to CI(G)S cells, though additional loss analysis was performed in conjunction with the stress tests described in a later section.

One loss analysis project done in conjunction with NREL (1/25/99 report to Contreras) was an analysis of the 18.8% record efficiency CIGS cell. Fig. 1 compares the current-voltage curves of this cell with the previous record CIGS cell (17.7%) and the highest-efficiency crystalline silicon

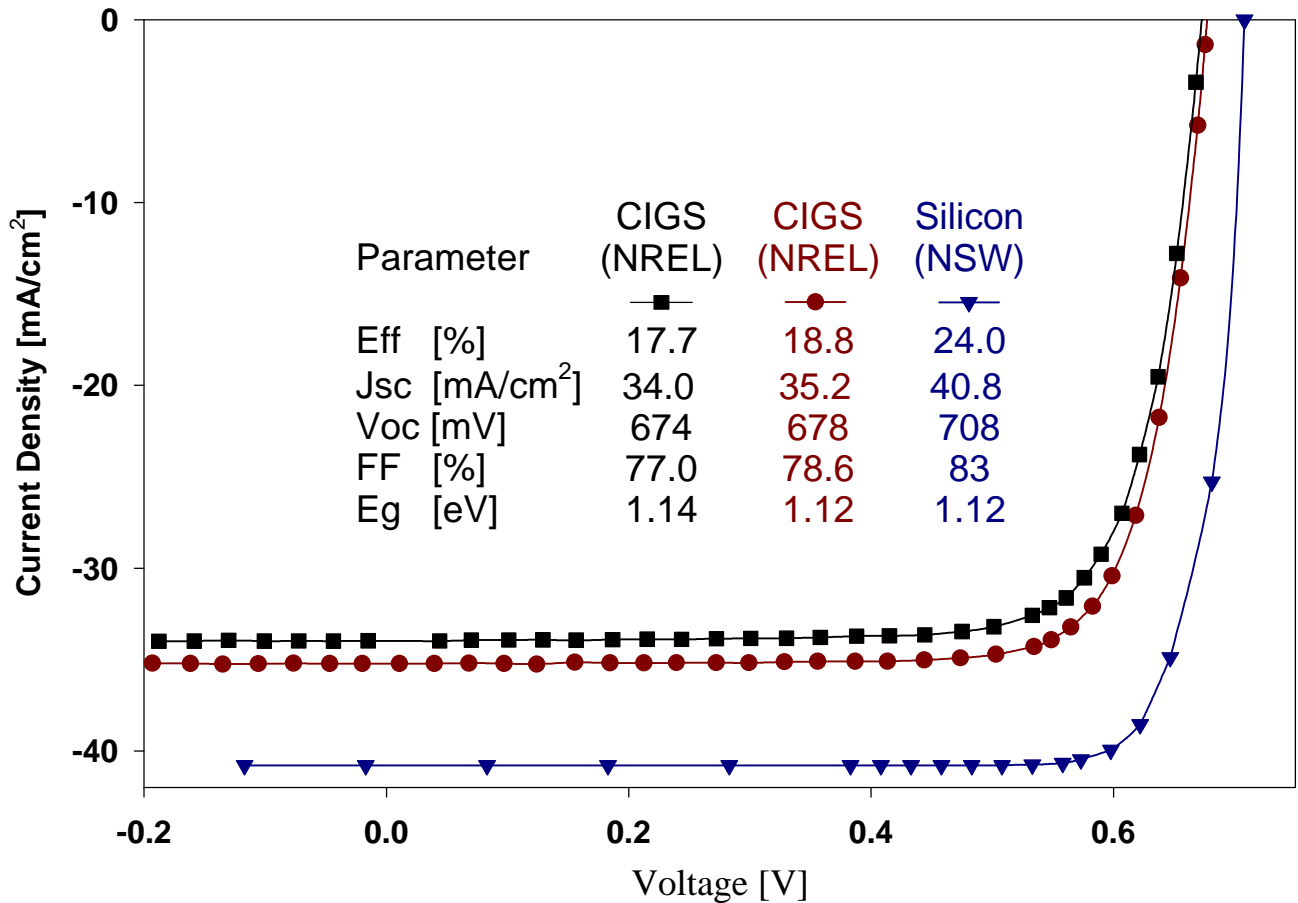


Figure 1. Current-voltage comparison of CIGS record cell, previous CIGS record cell, and record silicon cell.

cell (24.0%). From a direct comparison of quantum efficiency curves, we deduce that the new record CIGS cell has the same bandgap as silicon (1.12eV) while the earlier CIGS cell was slightly higher at 1.14 eV.

Table I illustrates the parameter-by parameter improvements from the previous to new record cell and the impact of each on efficiency. The last column gives the breakdown in efficiency

Table I. Comparison of previous and new record CIGS Cells

Comparison of NREL CIGS cells S773 and C1068				
<u>Parameter</u>	<u>S773</u>	<u>C1068</u>	<u>Change in Efficiency [%]</u>	<u>Adjusted for Bandgap [%]</u>
Efficiency	17.7%	18.8%	1.1	1.1
Bandgap	1.14 eV	1.12 eV	–	–
J_{sc}	34.0 mA/cm ²	35.2 mA/cm ²	0.6	0.2
V_{oc}	674 mV	678 mV	0.1	0.5
ff	77.0%	78.6%	0.4	0.4
R_s	0.3 [Ωcm^2]	0.2 [Ωcm^2]	$\left. \begin{array}{l} \\ \leftarrow \\ \leftarrow \\ \leftarrow \end{array} \right\} \begin{array}{l} 0.1 \\ 0.1 \\ 0.2 \end{array}$	$\left. \begin{array}{l} \\ \leftarrow \\ \leftarrow \\ \leftarrow \end{array} \right\} \begin{array}{l} 0.1 \\ 0.1 \\ 0.2 \end{array}$
r_s	3800 [Ωcm^2]	10000 [Ωcm^2]		
A	1.6	1.5		

improvement after correction for bandgap. The largest factor is an improvement in V_{oc} by 24 mV relative to the bandgap, or equivalently a reduction in the forward-current recombination current by 40%. Remarkably, the value of V_{oc} has reached 96% that of the best crystalline silicon. Also shown in Table I, the fill-factor has increased through a mixture of small improvements in series resistance R_s , shunting r_s and diode quality factor A. The current has also improved a small amount due to a slightly better red response, which probably implies a longer diffusion length.

A second CIGS project in collaboration with NREL (12/17/98 report to Bhattacharya) was the analysis of cells with absorber layers made by electrodeposition (ED) and by electroless solution

growth (EL). The goal was to investigate possibilities for low cost processes, and the results have been encouraging: 15.4% efficiency for the best ED cell and 12.4% for the best EL cell. Table II shows the parameter comparison with the record cell discussed above. Since the band gaps vary, one would again need to include this difference in direct comparison of V_{oc} and J_{oc} .

Table II. Comparison of ED and EL CIGS cells with record cell

Cell	ED-device	El-device	PVD-device
Ga/(In+Ga)	0.4	0.20	0.23
Area [cm ²]	0.418	0.418	0.432
V_{oc} [V]	0.666	0.565	0.678
J_{sc} [mA/cm ²]	30.51	33.27	35.2
V_{max} [V]	0.554	0.434	0.567
J_{max} [mA/cm ²]	27.8	28.6	34.5
FF [%]	75.6	66.1	78.6
r_{shunt} [Ω -cm ²]	2000	1000	10000
R_{series} [Ω -cm ²]	0.3	0.1	0.2
Ideality Factor [A]	1.8	2.5	1.5
Depletion width [μ m]	0.2	0.25	0.5
Hole density [cm ⁻³]	1×10^{16}	1.5×10^{16}	1×10^{16}
Band Gap [eV]	1.20	1.09	1.12
Efficiency [%]	15.4	12.4	18.8

A third NREL collaboration on CI(G)S was comparison between cells made with the standard CdS process and those without CdS, but with a Zn-solution treatment of the absorber surface prior to the deposition of the TCO front contact (11/2/98 report to Ramanathan). A summary of the parameter comparison is given in Table III, and again the results are promising in that the best CdS-free cells were similar to those fabricated with CdS on the same absorbers. There is some tradeoff, however, in that the CdS-free cells have higher J_{sc} , due to reduced window absorption, but lower V_{oc} . They also tend to have more current leakage, and may be somewhat less stable at present.

Cell comparison and loss analysis has also been done in collaboration with ISET (5/28/98 and 2/12/99 reports to Basol) where we evaluated the impact of process changes on current-voltage, capacitance voltage, and quantum efficiency curves. Similarly, we have been working with

Table III. Comparison of device parameters from CdS and non-CdS buffer layers

Cell	S1247-B23-2	S1247-D23-3	S1247-C14-4	S1248-B23-2	S1248-A14-5	S1248-B14-4
Comments	CIS/CdS	CIS/Zn treatment	CIS/Zn treatment	CIGS/CdS	CIGS/Zn treatment	CIGS/Zn treatment
Area	0.43	0.43	0.43	0.43	0.433	0.43
V _{oc} [mV]	0.46	0.41	0.42	0.59	0.55	0.56
J _{sc} [mA/cm ²]	31.9	32.5	33.0	33.5	36.5	35.8
FF	0.65	0.63	0.68	0.68	0.67	0.61
Efficiency	9.6	8.5	9.5	13.5	13.5	12.3
r _{shunt, light}	1000	170	350	1500	220	100
R _{series, light}	0.8	(0.2)	(0.1)	0.5	0.1	0.3
A, light	1.7	(1.9)	(1.7)	2.0	2.0	2.2
r _{shunt, dark}	3000	250	570	3600	430	180
R _{series, dark}	0.8	(1.4)	(0.1)	0.6	0.1	0.1
A, dark	1.8	(1.6)	(1.7)	2.2	1.8	2.1
Depletion width	0.3	0.27	0.25	0.23	0.23	0.15
Hole density	1.7 x 10 ¹⁶	1.0 x 10 ¹⁶	1.0 x 10 ¹⁶	3.0 x 10 ¹⁶	1.5 x 10 ¹⁶	3.5 x 10 ¹⁶

colleagues at Siemens, WSU, and IEC (2/16/99 report to Olsen) in another project to compare CIGS cells made with and without a CdS layer.

A final area of loss analysis has focused on the optical effects from different TCO layers. We did a series of reflection and transmission measurements, and also deduced absorption from these, on samples of ITO made at MRG (7/29/99 report to Wendt). We did similar measurements and analysis on ZnO₂ layers deposited at ISET (9/23/98 report to Basol).

IMPURITY EFFECTS

Studies of impurity effects during Phase I concentrated on the role of sodium in CIS and CIGS cells. A comprehensive description of this work is found in the Ph.D. thesis of Jennifer Granata, and a summary will be given here.

Sodium was added to CIS and CIGS absorber layers in controlled amounts by coevaporation of NaSe₂ with Cu, In, and Se using NREL's physical-vapor-deposition facilities. In each case four Mo-coated substrates were used: (1) soda-lime glass (SLG) (2) soda-lime glass coated with SiO₂, (3) Corning 7059 borosilicate glass, and (4) alumina. The first substrate allowed sodium to reach the CIS because of diffusion through the Mo, the second attempted to block sodium diffusion, and the latter two were nominally sodium free. Inductively-coupled plasma spectroscopy (IPS) and secondary-ion mass spectrometry (SIMS) were used to evaluate the amount and profile of sodium incorporation in the absorber layer. The actual concentrations ranged from about 1 ppm to a few per cent.

Fig. 2 shows current-voltage curves for varying amounts of sodium in CIS deposited on SLG/Mo and on alumina/Mo. In both cases, there is a distinct improvement with modest amounts of NaSe₂ and major deterioration if a large amount is used. The initial curve for the Na-free alumina substrate, however, is distinctively inferior to that of the sodium-containing SLG substrate. The low current of the 20-mg curve for alumina is due to other factors.

The largest sodium impact, excepting the very high concentration levels, is on the cell voltage (Fig. 2). In Fig. 3, V_{oc} for the six sodium concentrations on each of the four substrates is plotted against the average sodium concentration of the CIS layer, which includes both that diffused from the substrate and that added in the deposition. There is scatter in the data, but the overall trends are clear. The voltage increases with modest amounts of sodium, has a broad plateau between 0.01 and 0.1 at% but decreases above 1%. The decrease in voltage with large amounts

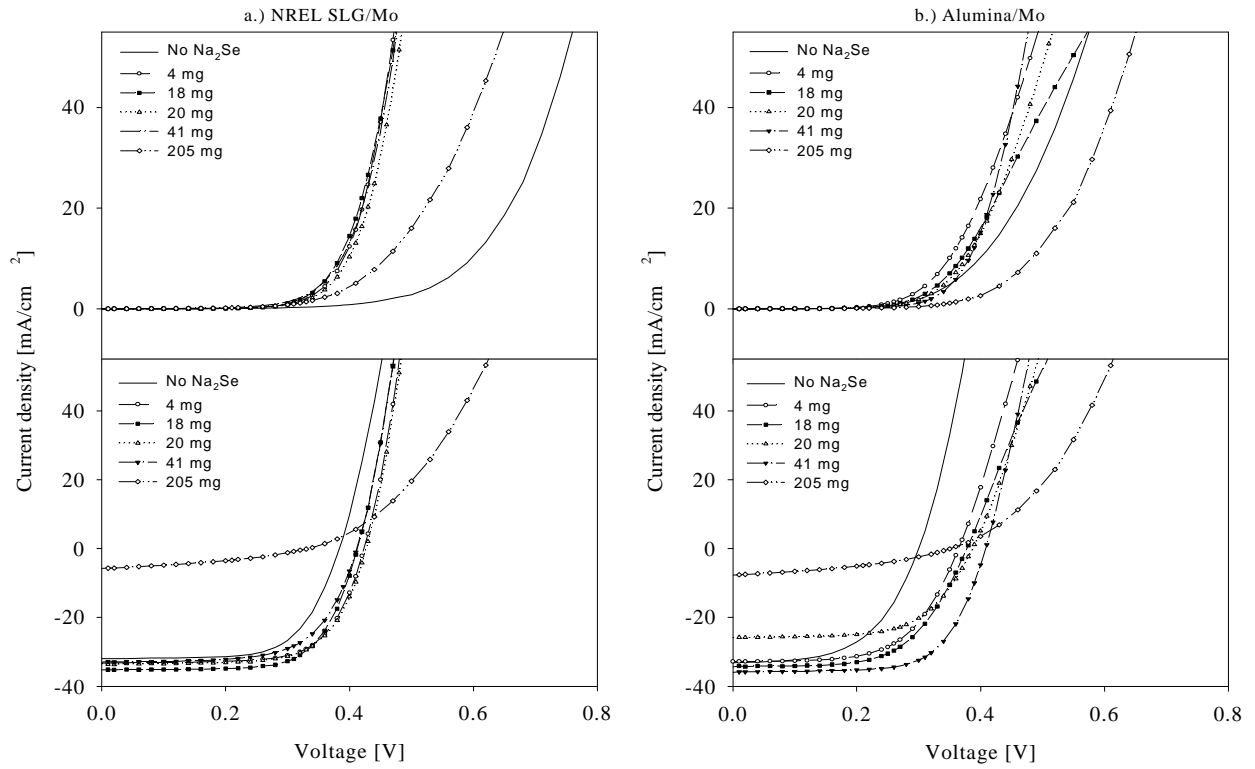


Figure 2. Current-voltage curves for varying sodium concentration. Two substrates.

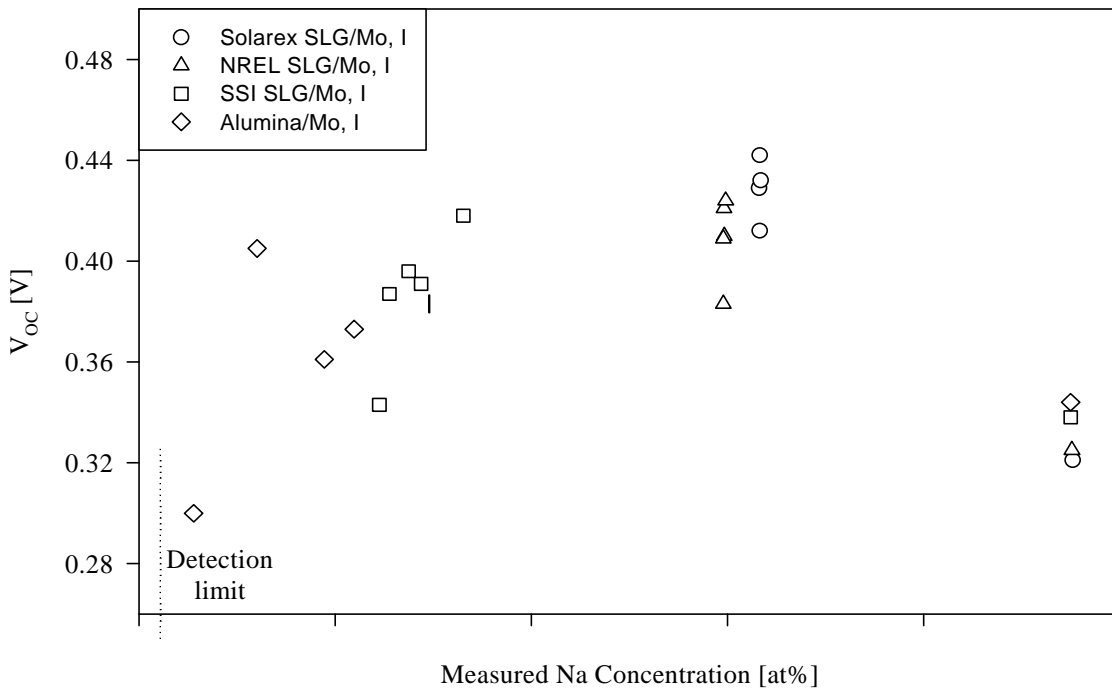


Figure 3. Sodium impact on V_{OC} using different substrates.

of sodium is accompanied by major decreases in current, especially in the red, and fill-factor as seen in Fig. 2. In this Na-concentration region, the CIS layer consists of smaller grains and is much more porous.

The variation of a second key parameter, the average CIS hole density derived from capacitance measurements, with sodium concentration is shown in Fig. 4. In this case, the hole density is near 10^{15} cm^{-3} for sodium concentrations of 0.01 at% and below, increases to the 10^{16} range for 0.1 – 1 at% and becomes very large for higher concentrations where the morphology changes are observed.

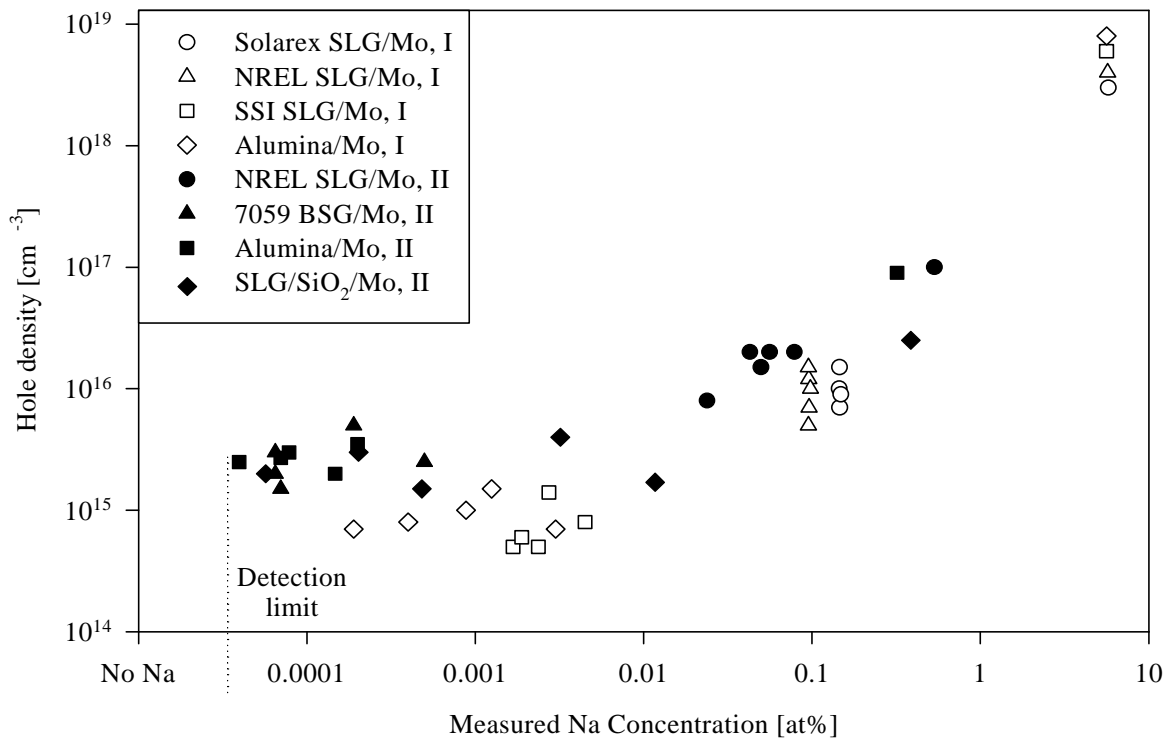


Figure 4. Variation in hole density with sodium concentration.

Improvements in CI(G)S cell performance with sodium addition have been seen by several groups, but there has not been agreement on the mechanism responsible. We believe it is a grain boundary effect, because (1) there is direct auger evidence of Na at the boundaries, but not in the bulk crystallite, (2) SIMS shows more total Na present with small-grained material than large, (3) increased V_{oc} implies less forward-current recombination, which is assumed to be primarily

determined by grain boundary states, and (4) increased hole density implies reduced compensation, also associated with grain boundary states.

Assuming, however, that the sodium responsible for better performance resides at the grain boundaries, there are at least three possible mechanisms: (1) It may directly help passivate the granular surface by reducing the number of uncoordinated In bonds. (2) It may indirectly passivate the surface by acting as a catalyst for oxygen, which would passivate the uncoordinated In bonds. (3) It could act as a surfactant during growth to inhibit formation of structures with compensating states or would yield generally larger crystallites. Future work should include systematic oxygen background control, variations in the sodium effect with gallium concentration, and similar investigations of impurities other than sodium.

SMALL-SPOT MEASUREMENT

A major new piece of apparatus has been constructed by Jason Hiltner, with assistance from David Warner, to allow local measurements of cell performance on a $1\ \mu\text{m}$ distance scale. The basic apparatus, shown in Fig. 5, consists of a solid-state laser source, fiber-optic transmission to shape the beam, beam expansion and digital attenuation, and beam alignment with four degrees of freedom onto an objective lens.

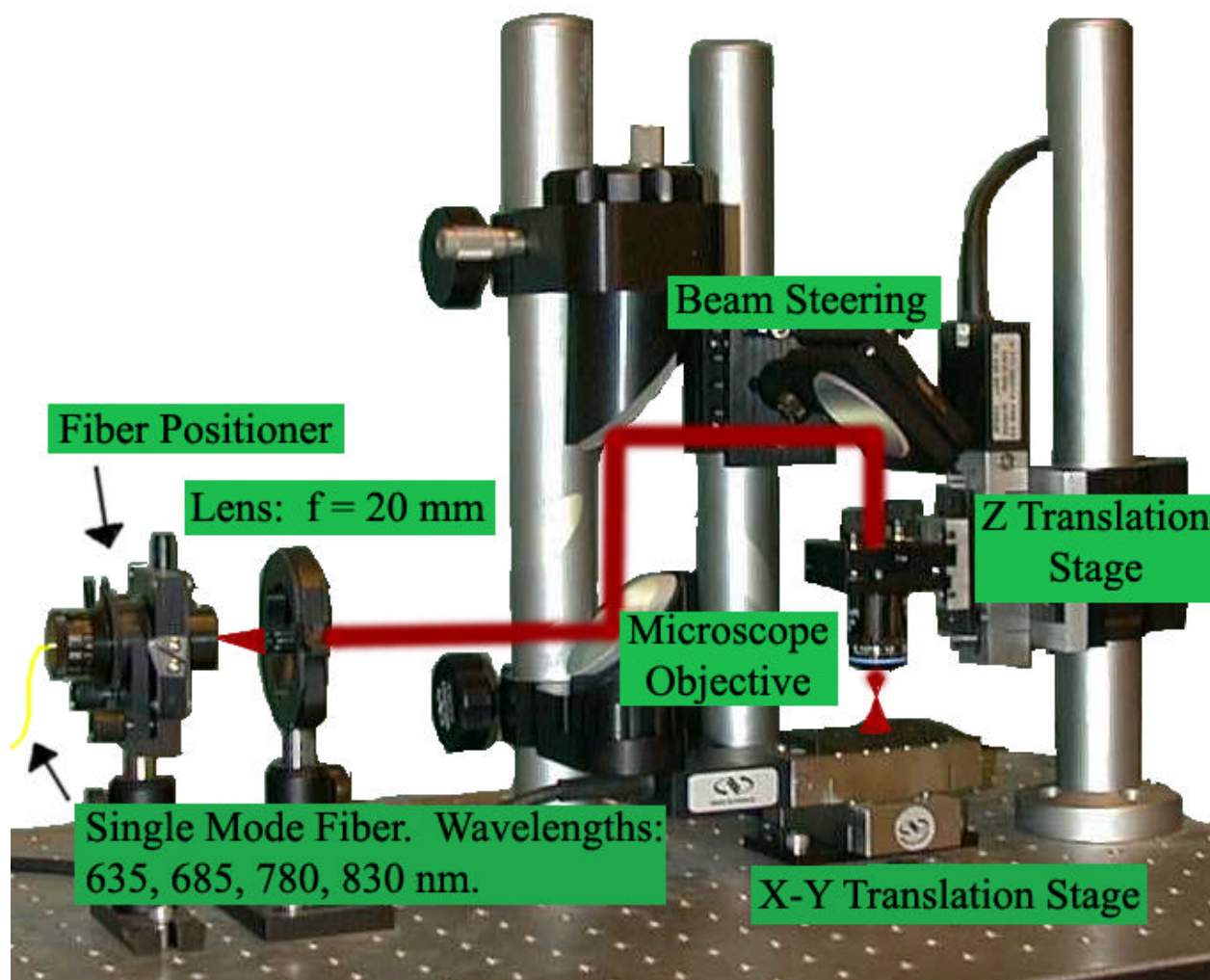


Figure 5. Small-spot measurement apparatus.

The 40X objective lens has a numerical aperture of 0.55 and 9 mm of working distance. It has adjustable compensation for focusing through glass, needed for use with CdTe cells. By

adjusting the Z-stage the spot striking a cell can be varied from 1 μm to 1 mm with excellent reproducibility. The laser can be chopped electronically, so that lock-in detection can be used.

Fig. 6 (top) shows the response when a CIS cell, illuminated through the slit between two razor

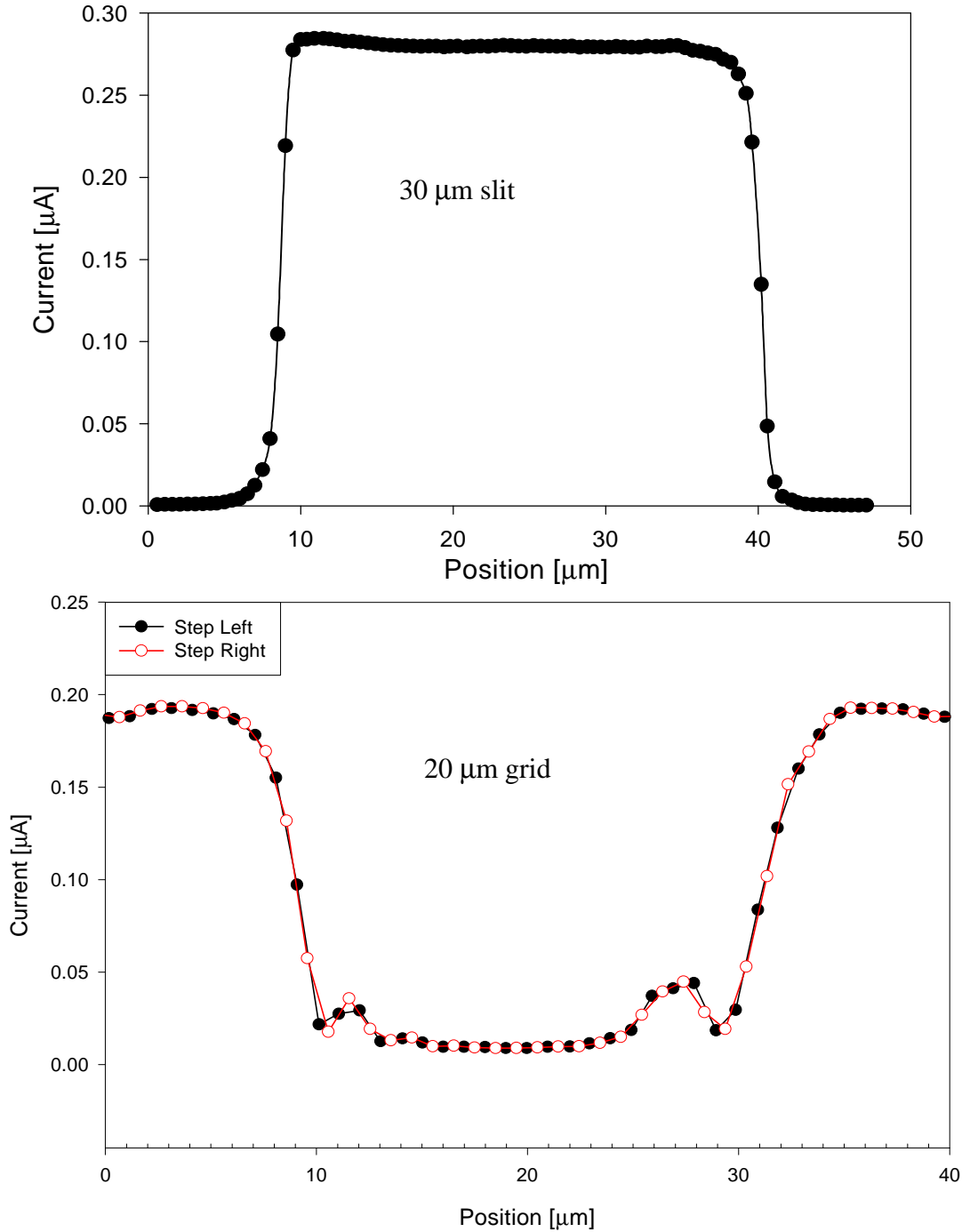


Figure 6. Small-spot CIS response stepped across a slit (top) and grid line (bottom).

blades is stepped through the beam. The cutoff on each side has a $1/e^2$ half width of approximately $1\ \mu\text{m}$ and the beam intensity at cell junction is about 100 suns. The bottom part of Fig. 6 shows the opposite situation where a similarly focused beam is scanned across a grid line. The structure is due to a finite width of the grid's optical cutoff and to reflective effects near the grid edges. This structure is useful to show the reproducibility of the system: the two types of data points correspond to two scans, one to the right and one to the left. Clearly, any backlash in the system is negligible. In fact, two dimensional scans over similar dimensions also give response profiles that are reproducible on a scale of less than a micron.

High intensity light spots, such as those used in Fig. 5, can induce a solar-cell response not indicative of that found under normal operating conditions, so the intensity of the $1\ \mu\text{m}$ spot was systematically attenuated down to near 1 sun (see Fig. 7). Even at the lowest intensities, where

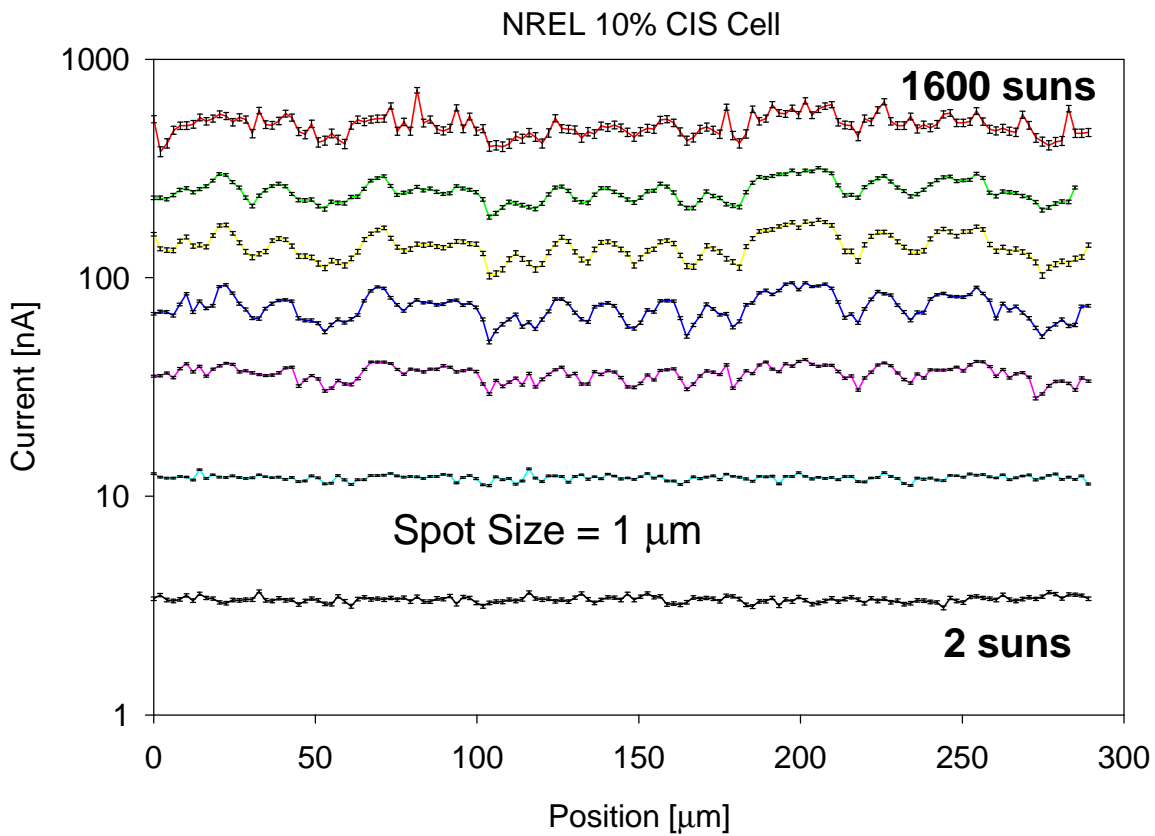


Figure 7. Small-spot stepping scans at several intensities.

the photocurrent is only a few nA, there is relatively little fluctuation in the measured response. The apparent fluctuations at higher intensities are in fact real and reproducible. They represent variations in local resistance and will be a useful tool for future work.

The power of the small-spot stepping apparatus should become apparent in the next Phase of the project. There is considerable evidence, including features seen in Fig. 7, that polycrystalline solar cells do not have a uniform response. The performance generally reported is an average which must therefore include a range of efficiencies from different regions. If we can identify and analyze the regions of low response, there will be a realistic possibility of eliminating them. Furthermore, when changes are induced in cell response, either deliberately or not, response details can be examined on a microscopic scale before and after the changes.

STRESS TESTS

Both CdTe and CIS cells have been tracked for periods of time under elevated temperature in the light and dark and at varying bias conditions. Collectively, we refer to these experiments as stress tests or accelerated life tests. They are designed to give information on what to expect from cells exposed to normal operating conditions for much longer periods of time. During Phase I, such tests were conducted on cells from Solar Cells, Inc. (now First Solar), NREL, and the German company ANTEC.

Fig. 8 shows the light and dark current-voltage curves for one CdTe cell. The measurements were taken at room temperatures, but between measurements the cell was held at 100° C under approximately two sun illumination and zero voltage. Changes were measured at three temperatures to establish an activation energy, which implied an acceleration of roughly 1000 in rate of change compared to the integration of measured temperatures at NREL. Hence, 37 days corresponds to roughly 100 years in the field.

The primary change seen in Fig. 8 is an increase in series resistance. Typically, such decrease in fill factor is the first effect to be seen, followed by decrease in voltage, and in extreme cases by lower photocurrent, particularly in the red. The degree of change illustrated by Fig. 8 varies considerably with fabrication details, particularly those related to the back contact, and with the electrical bias condition. Generally, the change is greater (11/5/98 report to NREL) when the cell is at open-circuit or higher forward bias or at a similar magnitude reverse bias. It also seems to be larger (11/9/98 report to NREL) when more copper is used in the contacting process.

Copper in fact is the primary suspect when there are stability problems with CdTe cells. It is used to form a p⁺⁺ or metallic-alloy layer on the back surface of CdTe, and it greatly facilitates a low-resistance contact, but copper is also a fast diffuser. As such, it appears with time to diffuse both away from the back contact, leaving it less ohmic, and towards the primary diode

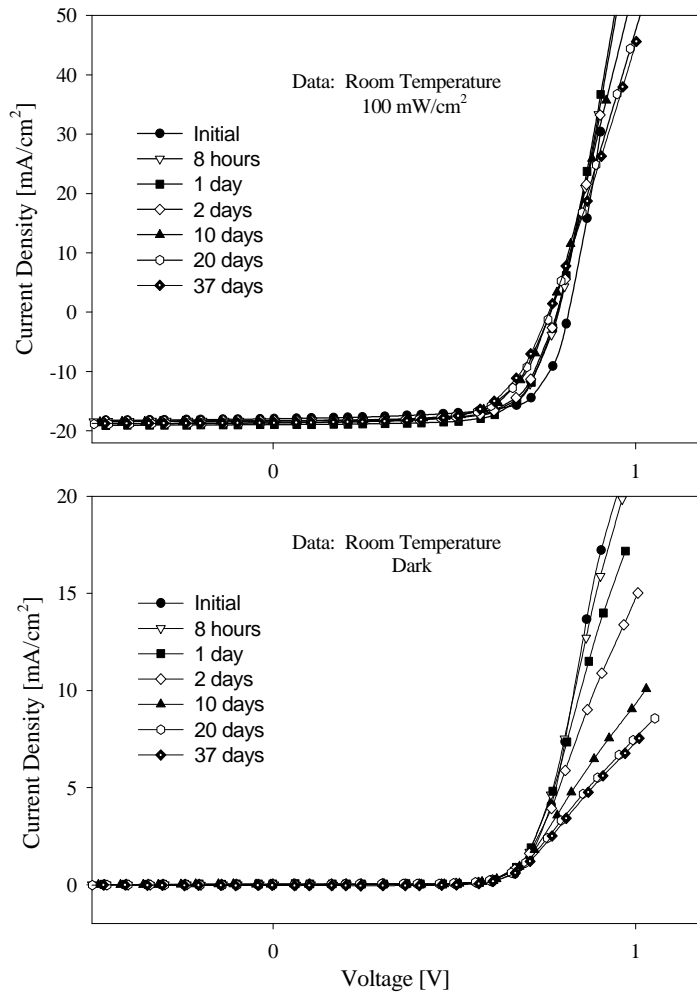


Figure 8. Light and dark current-voltage curves following illumination at 100°C for varying time periods.

junction, decreasing its effectiveness. Further work is needed on minimizing this issue by either better stabilizing the copper or going to a copper-free contact.

Fig. 9 shows the changes in capacitance for the same cell used for the J-V curves in Fig. 8. It shows that the capacitance vs. voltage curve is becoming increasingly flat, which corresponds to a progressive decrease in hole density, approaching complete depletion of the CdTe. The steep increase in hole density at $2 \frac{1}{2} \mu\text{m}$ denotes the physical boundary between CdTe and the back contact materials.

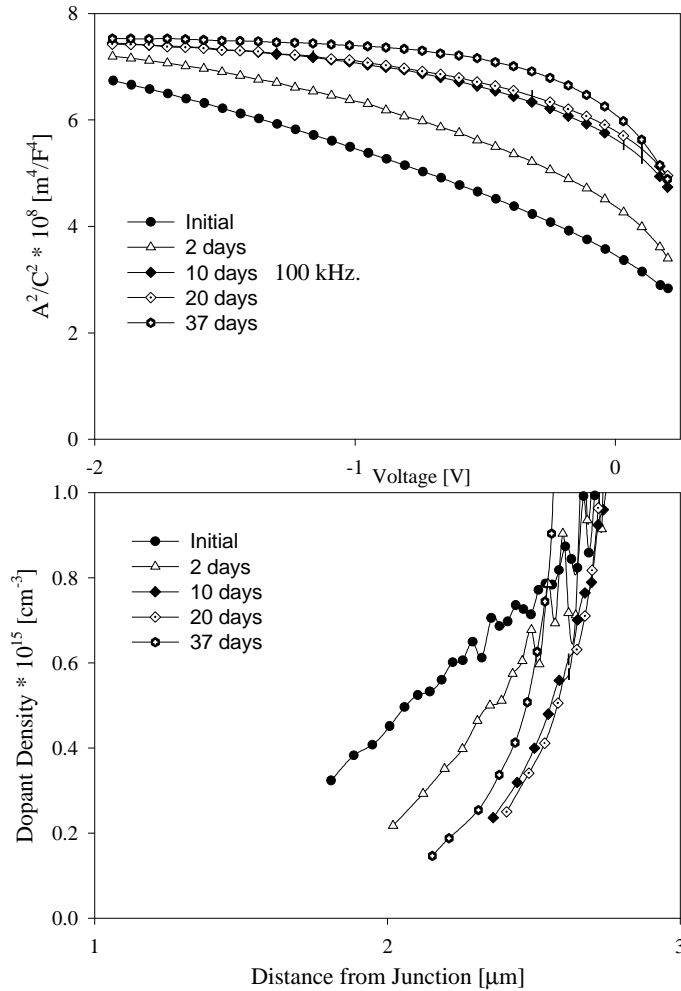


Figure 9. Changes in capacitance with temperature stress (top) and resulting hole density (bottom).

Stress tests done on Siemens CIS cells yield distinctly different results than the CdTe cells described. With the Siemens cells, the effects are more reversible, and are referred to as transients. Efficiency, driven primarily by the fill factor, decreases at high temperatures in the dark, but is restored under illumination. The upper part of Fig. 10 shows the fill factor after 20 hour alternating exposures to elevated temperature in the dark and to illumination. The bottom part of Fig. 10 shows that the recovery under illumination is gradual. In fact, it is only about half complete, and more recent measurements show that after several days the cell is essentially restored to its initial condition.

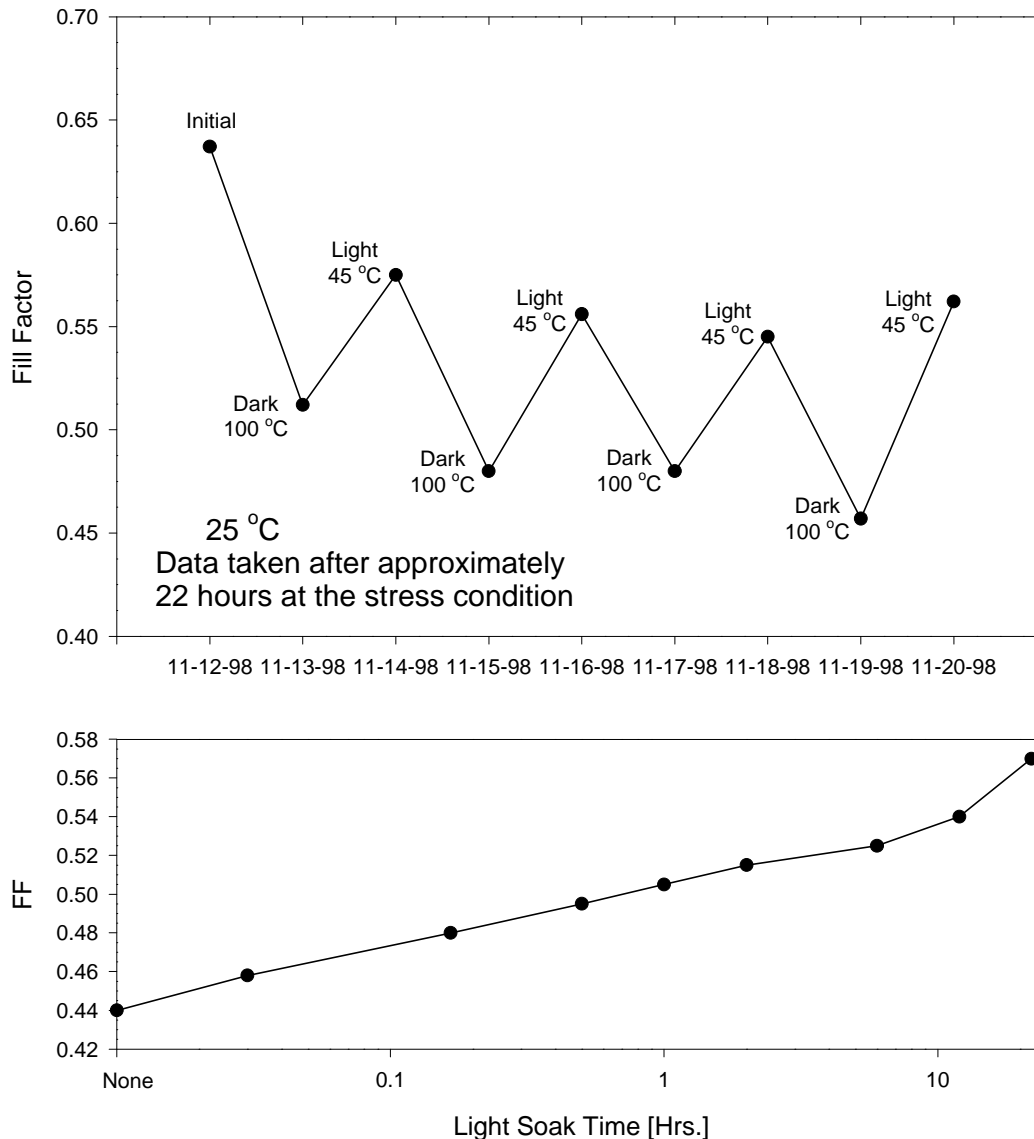


Figure 10. Siemens CIS fill-factor following dark and light stress cycles (top) and the more detailed recovery.

A final set of CIS and CdTe stress measurements was done at room temperature, but under increasing reverse bias. The purpose was to simulate conditions in a module where one cell might be partially shaded, and hence the other cells would force sufficient current through it to potentially cause damage. This project was assigned to undergraduate Yvonne Shelton, who will give a presentation at the Spring American Physical Society meeting. Results showed that in general both CIS and CdTe cells were sufficiently leaky that reverse currents similar to J_{sc} could pass through them at an induced reverse bias of a few volts.

MODELING

Modeling of CdS/CdTe cells began in earnest during Phase I. The work in this section was done by Alan Fahrenbruch using the AMPS software developed at Pennsylvania State University. Initial calculations used the layers shown schematically in Fig. 11. First calculations examined the effect of variations in the back contact potential Φ_c on the current-voltage curves. It was

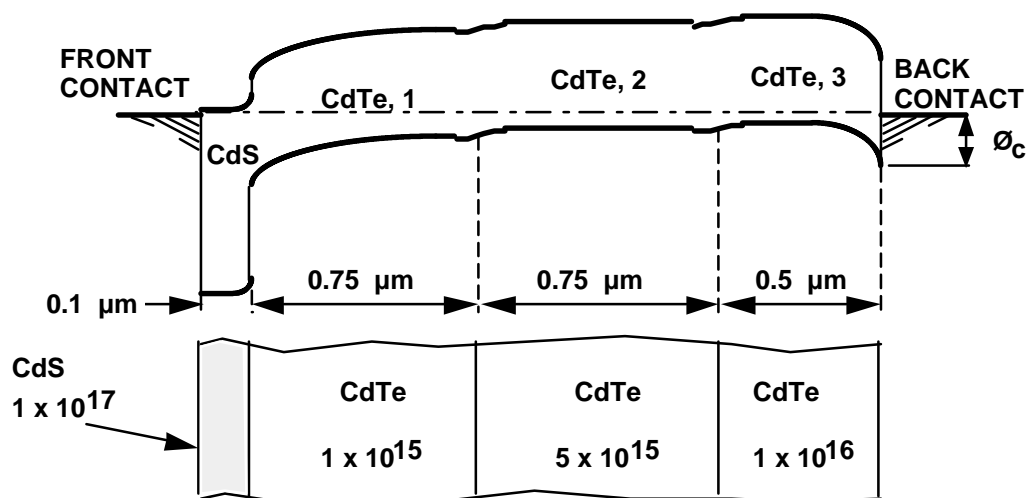


Figure 11. Initial modeling profile for CdTe calculations.

found that with increasing Φ_c , the first effect was current-limitation, or “roll over,” in the first quadrant, followed at larger values by distortion in the power quadrant and consequent reduction in fill factor.

These calculations also attempted to match credible cell parameters with the current-voltage curves of high-quality cells. The procedure worked well for J_{sc} and ff, but predictions for V_{oc} were consistently higher than those found in actual cells. Hence, an additional mechanism is strongly suggested, and the next step will be to add a layer of CdTe with considerably reduced lifetime near the CdTe interface. Such a layer would be consistent with growth morphology which shows much smaller grains near the interface. At the same time it is likely that the rest of the CdTe can be effectively modeled with a single carrier density.

A second, and very significant, part of the modeling effort has been to capture the inherently two-dimensional aspects of a polycrystalline solar cell without unduly complicating the problem. The top part of Fig. 12 shows a realistic schematic of a typical CdTe cells. The TCO is flat, the CdS is granular, the CdTe grain boundaries are primarily moved to the original surface, and there

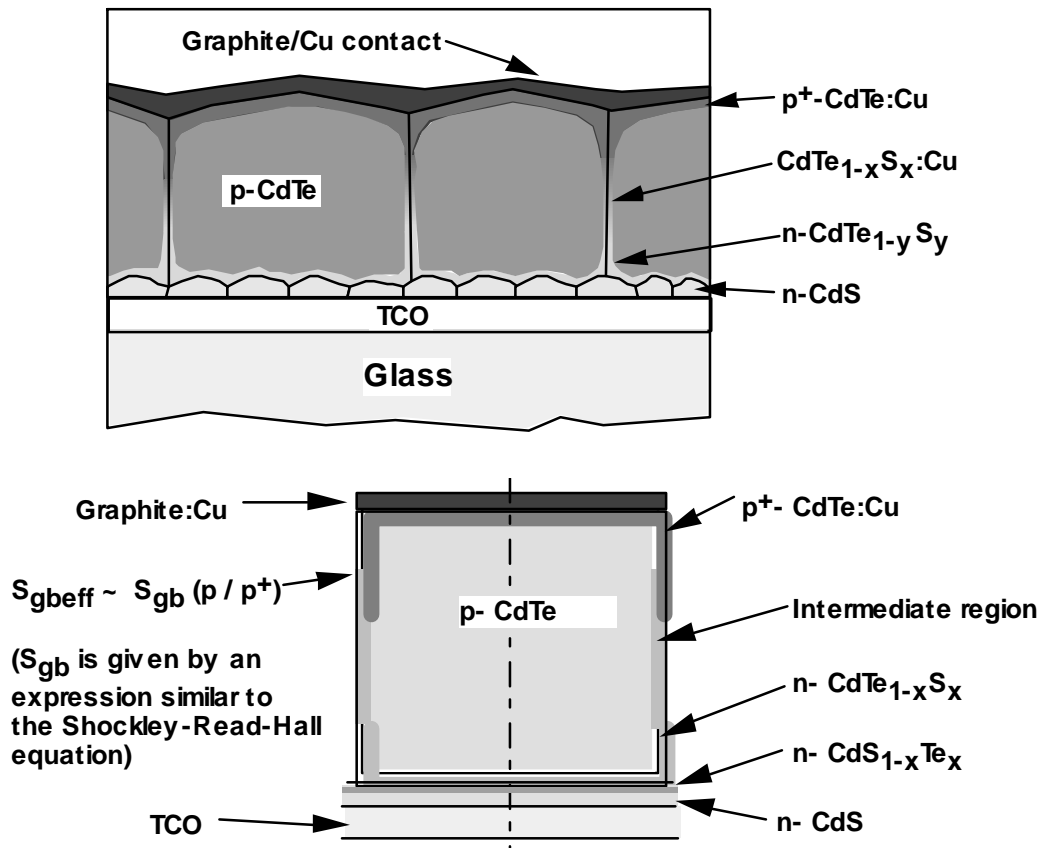


Figure 12. Schematic of CdTe cell profile (top) and further abstracted grain boundary for modeling.

is extension of both the CdS/CdTe and back-contact interfacial regions along the CdTe grain boundaries.

The bottom part of Fig. 12 shows a further, but still realistic abstraction of the problem. The strategy is to first solve the problem for the simplified simple grain and then calculate the total

current from a spectrum of grain sizes, which when treated in parallel form a reasonable approximation of the solar cell.

Two other issues which should be amenable to straight-forward modeling are the known interdiffusion of CdS and CdTe and the common use of a high-resistivity TCO layer. In the first case, the mixed CdS/CdTe regions will alter both the bandgap profile and the likely density of recombination states. In the second case, there will be additional buffering of the cell's junction from the front contact, which may well be the key to reduction or elimination of the CdS layer.

COMMUNICATIONS

Publications

1. “Blue-Photon Modification of Nonstandard Barrier in CuInSe₂ Solar Cells,” Solar Energy Materials and Solar Cells **53**, 367 (1998). I.L. Eisgruber. J.E. Granata.
2. “Losses Due to Polycrystallinity in Thin-Film Solar Cells,” Solar Energy Materials and Solar Cells **55**, 43 (1998). J.R. Sites, J.E. Granata, and J.F. Hiltner.
3. “Impact of Sodium in the Bulk and Grain Boundaries of CuInSe₂”, Proc. 2nd World PV Energy Conf., p. 604 (1998). J.E. Granata and J.R. Sites.
4. “Stability of CdTe Solar-Cells at Elevated Temperatures: Voltage, Temperature, and Cu Dependence,” AIP Conf. Series **462**, 170 (1998). J.F. Hiltner and J.R. Sites.
5. “CuIn_{1-x}Ga_xSe₂ Photovoltaic Cells from Solution – Deposited Precursor Films” submitted to Appl. Phys. Lett. R.N. Bhattacharya, W. Batchelor, J.R. Hiltner, and J.R. Sites.

Graduate Degrees

1. Jason Hiltner (M.S., May 1998) Coursework/Project Degree
2. Jennifer Granata (Ph.D., December 1998) Thesis: “The Impact of Deliberate Sodium Incorporation on CuInSe₂ Based Solar Cells.”

Specific Reports

<u>Date</u>	<u>To</u>	<u>Done By</u>	<u>Topic</u>
5/28/99	ISET/Basol	Johnson	Comparison of CIS Cells
7/29/98	GSE/Wendt	Granata	ITO Optics
8/21/98	SSI/Tarrant	Johnson	Dark/Light CIS Stress
9/7/98	CdTe Team	Hiltner	CdTe Stress Tests
9/23/98	ISET/Basol	Granata	ZnO Optics
11/2/98	NREL/Ramanathan	Granata	CdS vs. Zn-treatment
11/5/98	NREL/CdTe Group	Hiltner	Standard Contact Stress
11/9/98	NREL/CdTe Group	Hiltner	Varied Contact Stress
11/7/98	ANTEC/Bonnet	Hiltner	CdTe Stress Cycles
12/2/98	SSI/Tarrant	Granata	CIS Stress Cycles
12/17/98	NREL/Bhattacharya	Hiltner	ED and ED CIS Cells
1/25/99	NREL/Contreras	Hiltner	Record CIGS Cells
2/12/99	ISET/Basol	Hiltner	Cu- vs. In(Ga)-rich CIGS
2/16/99	WSU/Olsen	Hiltner	CdS/non-CdS Comparison